

Permanent magnets for water-scale prevention

Lipus, L.C.^{a,*}, Hamler, A.^b, Ban, I.^c, Acko, B.^a

^aFaculty of Mechanical Engineering, University of Maribor, Maribor, Slovenia

^bFaculty of Electrical Engineering and Computer Science, University of Maribor, Maribor, Slovenia

^cFaculty of Chemistry and Chemical Engineering, University of Maribor, Maribor, Slovenia

ABSTRACT

Anti-scale magnetic treatment (AMT) is discussed with the emphasis on the construction of magnetic devices and the mechanism of AMT influence on scale formation. Two field cases are reported of mineral-fouling reduction during water heating by using permanent magnets. Instead of hard encrustation on the heated surfaces a powdery deposit was formed because of modified crystal morphology (observed by X-ray powder diffractometry and scanning-electron microscopy). In order to find a proper design for magnets regarding the influencing parameters (a magnetic-field distribution with alternating lines orthogonal to the water-flow and minimal density peaks 0.2 T), cost-effective for actual water-flow capacities, several models with NdFeB magnets were simulated by the finite-element method using the OPERA 15R1 computational program. Two optimized models are presented for moderate capacities: a model with a rectangular gap (a two-row set of rectangular magnets) for capacities from 0.5 m³/h to 3 m³/h, and a model with annular gap (annular magnets on a pipe and disk magnets within a cylindrical kernel) for 3.5 m³/h to 5.5 m³/h.

© 2015 PEI, University of Maribor. All rights reserved.

ARTICLE INFO

Keywords:

Scale control
Calcium carbonate
Magnetic water treatment
Permanent magnets
Modelling

*Corresponding author:

lucija.lipus@um.si
(Lipus, L.C.)

Article history:

Received 30 January 2015
Revised 16 November 2015
Accepted 20 November 2015

1. Introduction

Mineral fouling is a frequent technological problem during water processing. Encrustation in pipelines reduces the flow capacity, thus requiring more pumping power. When precipitated on heated surfaces it additionally reduces the heat-transfer owing to the insulating effects of the minerals. The predominant scale from ground and terrestrial waters is calcium carbonate owing to its decreasing solubility with CO₂ gas released from the solution when the temperature is increased (e.g. in heat-exchangers) or the pressure is reduced (e.g. during water spraying or in a geothermal well). Its solubility also depends on the *pH*: for instance, when NaOH is added CO₂ forms additional carbonate ions and the precipitation of CaCO₃ occurs. Depending on water processing conditions, CaCO₃ commonly precipitates in amorphous and various crystalline modifications: rhombus-shaped calcite that may adhere into highly-compact scale; needle-like aragonite that tends to form a brittle scale, but in rigorous thermal and hydrodynamic conditions grows into a hard scale, and spherical vaterite that usually form a powder-like scale.

Economic and environmental concerns have led to the development of alternative physical means for hard-scale prevention: by the usages of permanent magnets [1-5], electromagnetic coils [6-9], electrodes [10, 11], and ultrasonic pretreatment [12]. The common principle of these treatments is the pre-precipitation of calcium carbonate (a homogenous nucleation/coagulation in bulk water) into fine suspended particles that later in critical regions (e.g. under the hot con-

ditions of the heat-exchanger) offer preferable surfaces for crystallisation, depositing as a loosely adhered sludge or being carried further by the water-flow.

Here a modelling of NdFeB magnets for particular water-flow capacities is presented, and certain experiences with field applications are briefly reported. As such treatment does not change the composition of water it is convenient for the food industry, and drinking water installation.

2. Operating principle of the magnetic water treatment

The anti-scale magnetic treatment of hard water has been employed for more than half a century, but the application has sometimes proved to be ineffective due to insufficient data about efficiency requirements [13] and still some influencing factors are unrecognized [14]. The phenomenon is not related to the magnetic-force action on dispersed particles [15]. Summarizing the explanations proposed, the mechanism comprises at least two types of interactions influencing the interfacial processes: magnetically modified hydration of ions and interface surfaces [16, 17], and Lorentz-force action on ions at electrically charged particles [18].

Experimental research under well-controlled laboratory conditions and several field tests under real long-term conditions have been done. A systematic test with artificial solutions passed through a magnetic field (magnetic flux density 0.16 T, exposure time 15 min, at different flow rates of 0.54-0.94 l/min) showed an increase in the total precipitate quantity and in the formation within the bulk solution (instead of incrustation on the walls), but this was strongly dependent on the physicochemical properties of the surface material [1, 2]. There are also other reports that dynamic magnetic treatment (i.e. where water flows through the magnetic field) can be effective at maximums as low as 0.1 T to 0.2 T [3, 19, 20]. The effectiveness of a row of permanent magnets (producing magnetic-field orthogonally to the water-flow) increases, whilst increasing the flow rate (up to 1.8 m/s); and the alternating distribution of the magnetic field seems more effective than in the case of non-inverted permanent magnets [19]. In field applications, magnetic devices are constructed for water-flow velocity, commonly 1 m/s to 2 m/s. The exposition time practically 0.03 s to 1 s at 0.05 T to 0.25 T was taken for hard-scale prevention [21, 22]. In a large-scale test [23], the exposition at 0.15 T was close to 0.1 s. There are some reports about high energy savings, reduced cleaning and process down-time costs, owing to the installations of such devices [24-27].

Furthermore, since magnetic treatment offers a variety of selective influences on different substances and processes, these magnetic devices have much wider possibilities for usage, e.g. during coagulation [28], filtration [29], textile treatment [30, 31], redox [32] and enzymatic processes [33], even fuel combustion [34].

3. Field tests

A self-constructed magnetic device (presented in Fig. 4b) yielded some changes in scale thickness formed the high-temperature heating condition [5, 35], but it proved to be more efficient in various field heat-exchangers in which water was heated maximally to 60 °C. Two cases are reported here. The scales were observed using an AXS-Baker/Siemens/D5005 X-ray Powder Diffractometer, and a FEI – QUANTA 200 3D Environmental Scanning Electron Microscope.

A scale-prevention test: 3 m long hot (close to 80 °C) horizontal pipes in a 5 m high container were cooled by pouring groundwater (0.6 m³/h, total hardness 25 dH and an outlet temperature close to 40 °C). The encrustation that drastically reduced the heat-transfer predominantly consisted of calcite and goethite FeO(OH) (Fig. 1a). After the surfaces had been mechanically cleaned up, a magnetic device (0.18 m long), was installed onto the cooling-water input: only a smaller amount of powdery aragonite (Fig. 1b) accumulated on the upper surfaces and was washed away periodically by a water-jet.

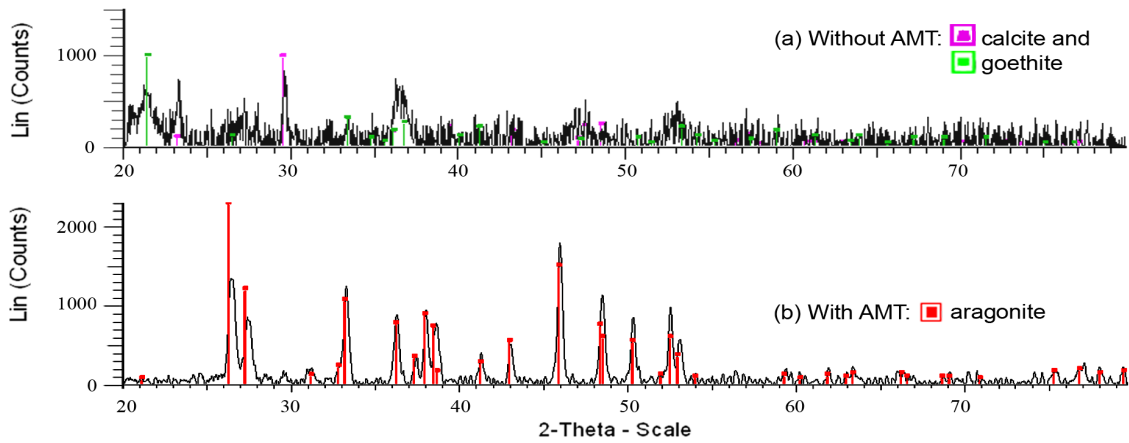


Fig. 1 X-ray diffraction spectrographs of scales from the scale-prevention test

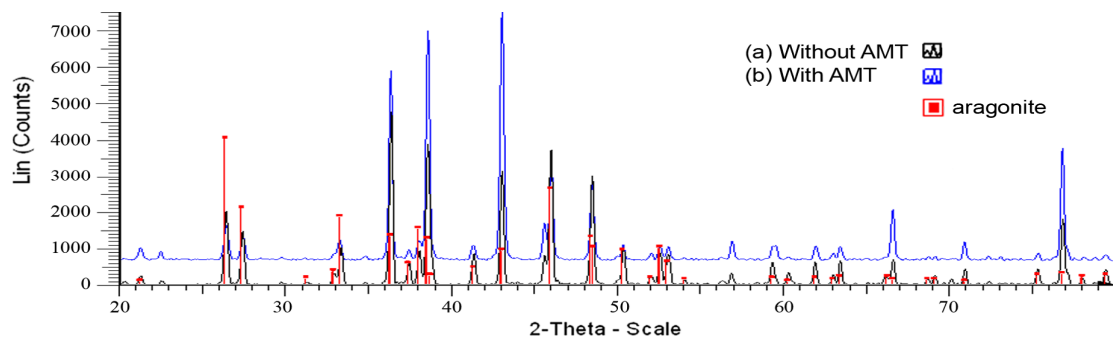
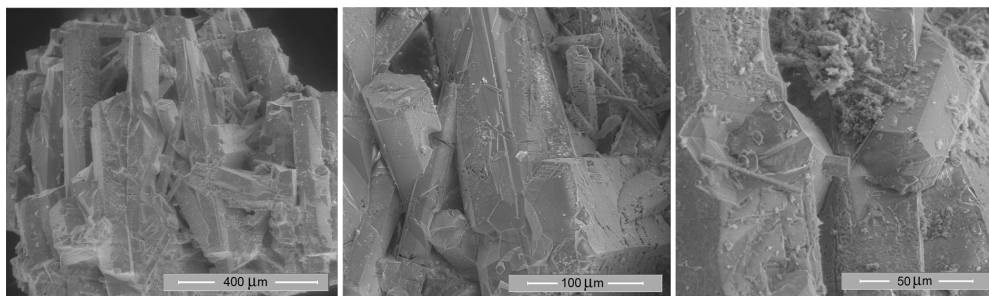
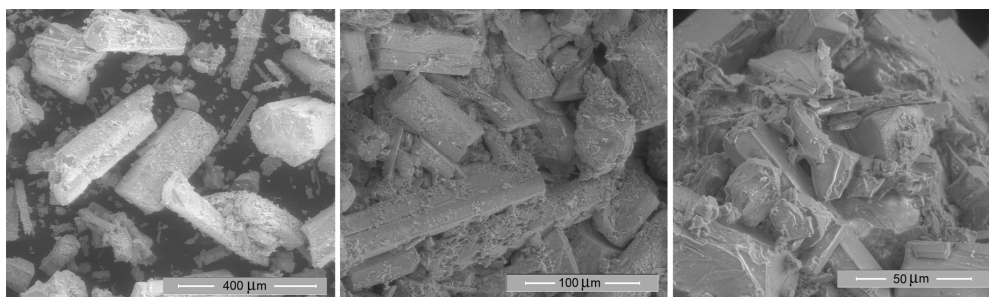


Fig. 2 X-ray diffraction spectrographs of scales from the scale-removal test



(a) Without AMT: A particle broken from porous compact scale



(b) With AMT: A powder of dried slime

Fig. 3 Micrographs of scales from the scale-removal test

A scale-removal test: the region around a sheaf of 12 mm thick spiral pipes of 1.7 m in length and a 3 dm thick cylindrical housing was blocked whilst heating the tap water (1.2 m³/h, total

hardness 17 dH, and an outlet temperature varying from 50 °C to 65 °C) by porous but compact aragonite (Figs. 2a, 3a, needles with predominant diameters of a few-tens μm). By applying the magnetic device (two parallel units, 0.24 m long) without previous mechanical cleaning, the scale was gradually converted into fine slime (Figs. 2b, 3b) and washed away by high-pressure water-flow.

4. Device construction

Different arrangements of permanent magnets were investigated and simulated to find a simple but efficient system for a particular water-flow capacity. After the preliminary dimensioning, the precise dimensions were sought in order to find the proper magnetic-field distribution and the required magnetic flux density, for which the computational program OPERA 15R1 (Vector Fields Software) was used with the finite-element operations [36, 37]. This method enables precise consideration of real 3D-geometry, taking into account the non-linearity of the magnetic properties of the construction materials, and the neighbouring poles' interactions. Since the conditions of the geometrically complex models cannot be determined directly, the geometry must be described by several divided simple geometric elements (i.e. finite elements), as the interference from these neighbouring elements must also be considered. The evaluation of the magnetic flux density along a chosen line or plane yielded local distribution. On the basis of these local distributions, a proper configuration for device construction was selected and then optimised by varying the following parameters: the thicknesses of the permanent magnets (i.e., the dimension orthogonal to the water-flow direction); the width (i.e. the dimension parallel to the water-flow direction); the direction of the magnets' magnetisation; the pipe diameter (which influences the distances between the magnets); the distances amongst the magnetic poles, and the thickness of the magnetic yoke. The aim of this procedure was to provide the orthogonality of the magnetic lines to the water-flow's direction and alternating orientation from peak to peak, and the following values recommended for efficient AMT: peaks of magnetic-field density, B , as high as possible, at least 0.1 T to 0.2 T; the water-flow velocity in the gap within the range from 1-2 m/s, and minimal exposure time from 0.1 s to 0.2 s.

Permanent NdFeB magnets (with a remaining magnetic flux density of 1.12 T and a coercive magnetic field intensity of 781 kA/m), available on the world market, are strong enough and thermally stable enough to use them for constructing such devices. Low-carbonic steel was selected for the material of the magnetic yoke. The casting was non-magnetic.

The alternating arrangement of rectangular magnets produced magnetic lines transversal to the water-flow. Simulation within the range 0.5-3 m³/h yielded a rectangular gap as an applicable solution. Results for selected water-flow capacities are summarised in Table 1 and the magnetic-field distribution for a particular case is presented in Fig. 4.

Table 1 Construction solutions for water-flow capacities $q_v = 0.5\text{-}5.5\text{ m}^3/\text{h}$ (D_{in} is inner diameter of the pipelining; r_{in} is inner radius of the annular gap; r_{out} is outer radius of the annular gap; v_1 is water-flow velocity the pipelining; v_2 is water-flow velocity in the gap of magnetic device).

Standard pipe	Model	Dimensions and water velocity	B peaks
$q_v = 0.5\text{-}0.7\text{ m}^3/\text{h}$ $D_{in} = 13\text{ mm}$, $v_1 = 1.1\text{-}1.5\text{ m/s}$	Fig. 4a Longitudinal magnetisation	$20 \times 20 \times 5\text{ mm}^3$ magnets, $18 \times 7\text{ mm}^2$ gap (1mm wall), $v_2 = 1.1\text{-}1.6\text{ m/s}$	0.2 T 0.4 T
	Fig. 4b Transversal magnetisation	$20 \times 20 \times 5\text{ mm}^3$ magnets, $18 \times 7\text{ mm}^2$ gap (1 mm wall), $v_2 = 1.1\text{-}1.6\text{ m/s}$	0.43 T 0.6 T
$q_v = 1.4\text{-}1.8\text{ m}^3/\text{h}$ $D_{in} = 20\text{ mm}$, $v_1 = 1.2\text{-}1.6\text{ m/s}$	Fig. 4c Transversal magnetisation	$25 \times 20 \times 5\text{ mm}^3$ magnets, $23 \times 12\text{ mm}^2$ gap (1 mm wall), $v_2 = 1.4\text{-}1.8\text{ m/s}$	0.3 T 0.4 T
	Fig. 4d Transversal magnetisation	$30 \times 20 \times 5\text{ mm}^3$ magnets, $28 \times 15\text{ mm}^2$ gap (1 mm wall), $v_2 = 1.5\text{-}2.0\text{ m/s}$	0.25 T 0.33 T
$q_v = 3.5\text{-}4.5\text{ m}^3/\text{h}$ $D_{in} = 30\text{ mm}$, $v_1 = 1.4\text{-}1.8\text{ m/s}$	Fig. 5 Annular gap	$r_{out} = 25\text{ mm}$ (1.75 mm wall), $r_{in} = 18\text{ mm}$ (1 mm wall), $v_2 = 1.0\text{-}1.3\text{ m/s}$	0.2 T
		$r_{out} = 24\text{ mm}$ (2.75 mm wall), $r_{in} = 18\text{ mm}$ (1 mm wall), $v_2 = 1.5\text{-}1.9\text{ m/s}$	0.4 T
$q_v = 4.5\text{-}5.5\text{ m}^3/\text{h}$ $D_{in} = 32\text{ mm}$, $v_1 = 1.5\text{-}1.9\text{ m/s}$			

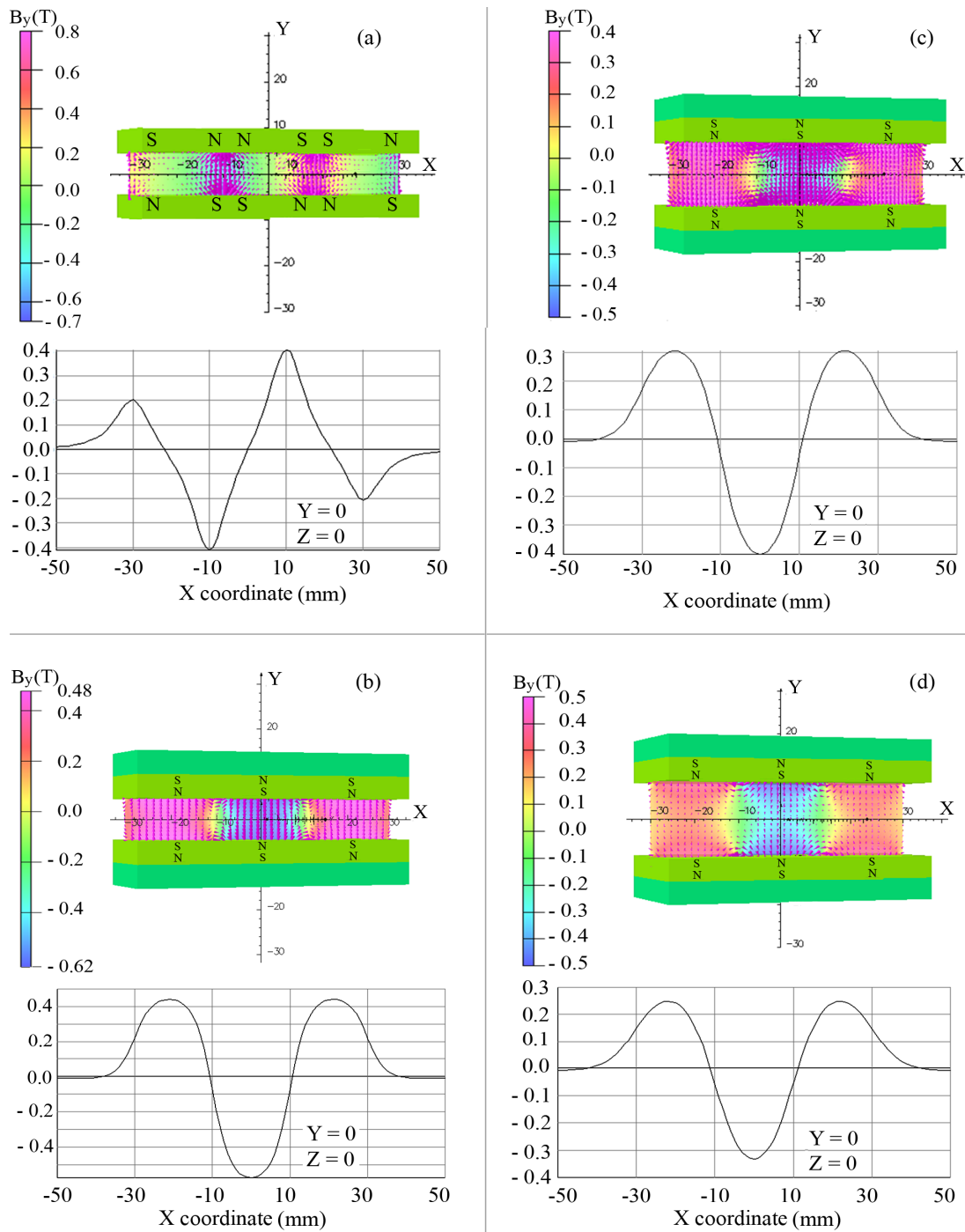


Fig. 4 Distribution of the magnetic-field within the rectangular gap (60 mm long) between two rows of rectangular magnets (three pairs) and the Y-component of magnetic- flux density along the axis of the gap, B_y .

The taken gap, a little wider than the inner-pipe’s diameter, provides velocity below the upper threshold, whilst the gap’s height optimises the magnetic-field’s strength and the hydrodynamic pressure loss.

The model with transversally-magnetized magnets (Fig. 4b) provides a stronger magnetic-field than in the case with the longitudinally-magnetised, at practically the same dimensions (Fig. 4a). In the cases with longitudinal magnetisation, the magnetic-field within the gap is strengthened by a ferromagnetic plate, which concentrates the magnetic flux. In contrast, the magnetic-field in the model with longitudinal magnetisation may be weakened by an eventually present ferromagnetic material in the vicinity of the magnetic device.

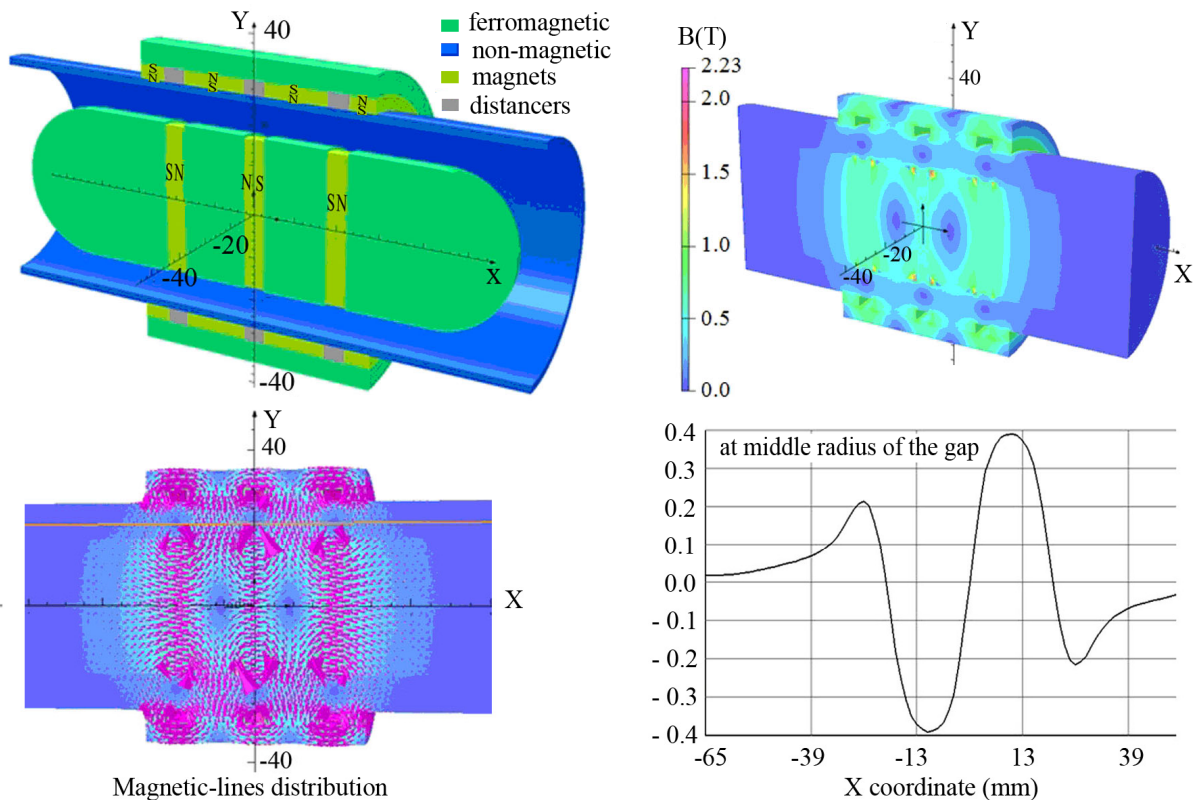


Fig. 5 Distribution of the magnetic field within the annular gap between a ferromagnetic kernel (with inserted disc magnets – three transversely-magnetised, with radii 17 mm and thickness 5 mm) and a 75 mm long ring (with inserted annular magnets – two rings with thickness 15 mm, two rings with thicknesses 7.5 mm and outer radii 30 mm).

The number of successive magnetic pairs is determined by the exposure-time requirement, e.g. 6 to 15 of pairs are needed in the case of 4b.

Water with flow capacities that are not presented in Table 1 can be treated by a parallel pair of smaller units (where the magnetic-field is stronger on account of higher hydrodynamic pressure loss) or by one bigger but weaker unit. In an extreme event, for instance, case 4d can also be applied for Pipe 2, where the water velocity in the gap is lower than the v_2 given in the table, thus requiring a smaller number of magnetic pairs, i.e. from 5 to 12.

The simulation within the range 3.5-5.5 m³/h yielded an annular gap as a hydro-dynamically more favourable solution. The system of annular and disc magnets is presented in Fig. 5.

5. Conclusion

Since magnetic treatment has a variety of selective influences on different substances and processes, its application has wide potentials.

Constructing a magnetic device for scale control at specific water-flow, some operational requirements, such as a sufficiently strong magnetic-field with proper flux distribution and a long exposure time, must be considered. This paper provided a review of models based on real operational data and material characteristics. For low capacities a model with parallel rows of transversely-magnetised magnets was proven to be a very simple solution; whilst for more than a few m³/h the model with narrow annular gap is more convenient for providing the required magnetic field at an acceptable pressure loss. The construction and installation is relatively easy, whilst the life-time is long and without any energy consumption.

Acknowledgement

We thank the Ministry of Higher Education, Science and Technology of the Republic of Slovenia for the financial support of the study, and the ABENA Company for manufacturing and field-testing the pilot devices.

References

- [1] Alimi, F.; Tlili, M.M., Ben Amor, M., Maurin, G., Gabrielli, C. (2009). Effect of magnetic water treatment on calcium carbonate precipitation: Influence of the pipe material, *Chemical Engineering and Processing*, Vol. 48, No. 8, 1327-1332, doi: [10.1016/j.cep.2009.06.008](https://doi.org/10.1016/j.cep.2009.06.008).
- [2] Alimi, F., Boubakri, A., Tlili, M.M., Ben Amor, M. (2014). A comprehensive factorial design study of variables affecting CaCO₃ scaling under magnetic water treatment, *Water Science and Technology*, Vol. 70 No. 8, 1355-1362.
- [3] Chang, M.C., Tai, C.Y. (2010). Effect of the magnetic field on the growth rate of aragonite and the precipitation of CaCO₃, *Chemical Engineering Journal*, Vol. 164, No. 1, 1-9, doi: [10.1016/j.cej.2010.07.018](https://doi.org/10.1016/j.cej.2010.07.018).
- [4] Stuyven, B., Vanbutsele, G., Nuyens, J., Vermant, J., Martens, J.A. (2009). Natural suspended particle fragmentation in magnetic scale prevention device, *Chemical Engineering Science*, Vol. 64, No. 8, 1904-1906, doi: [10.1016/j.ces.2008.12.022](https://doi.org/10.1016/j.ces.2008.12.022).
- [5] Lipus, L.C., Dobersek, D. (2007). Influence of magnetic field on the aragonite precipitation, *Chemical Engineering Science*, Vol. 62, No. 7, 2089-2095, doi: [10.1016/j.ces.2006.12.051](https://doi.org/10.1016/j.ces.2006.12.051).
- [6] Lee, S.H., Cho, Y.I. (2002). Velocity effect on electronic-antifouling technology to mitigate mineral fouling in enhanced-tube heat exchanger, *International Journal of Heat and Mass Transfer*, Vol. 45, No. 20, 4163-4174, doi: [10.1016/S0017-9310\(02\)00104-7](https://doi.org/10.1016/S0017-9310(02)00104-7).
- [7] Xing, X.K. (2008). Research on the electromagnetic anti-fouling technology for heat transfer enhancement, *Applied Thermal Engineering*, Vol. 28, No. 8-9, 889-894, doi: [10.1016/j.applthermaleng.2007.07.006](https://doi.org/10.1016/j.applthermaleng.2007.07.006).
- [8] Shahryari, A., Pakshir, M. (2008). Influence of a modulated electromagnetic field on fouling in a double-pipe heat exchanger, *Journal of Materials Processing Technology*, Vol. 203, No. 1-3, 389-395, doi: [10.1016/j.jmatprotec.2007.10.048](https://doi.org/10.1016/j.jmatprotec.2007.10.048).
- [9] Lipus, L.C., Ačko, B., Hamler, A. (2011). Electromagnets for high-flow water processing, *Chemical Engineering and Processing*, Vol. 50, No. 9, 952-958, doi: [10.1016/j.cep.2011.07.004](https://doi.org/10.1016/j.cep.2011.07.004).
- [10] Tijing, L.D., Kim, H.Y., Lee, D.H., Kim, C.S., Cho, Y.I. (2010). Physical water treatment using RF electric fields for the mitigation of CaCO₃ fouling in cooling water, *International Journal of Heat and Mass Transfer*, Vol. 53, No. 7-8, 1426-1437, doi: [10.1016/j.ijheatmasstransfer.2009.12.009](https://doi.org/10.1016/j.ijheatmasstransfer.2009.12.009).
- [11] Hasson, D., Sidorenko, G., Semiat, R. (2011). Low electrode area electrochemical scale removal system, *Desalination and Water Treatment*, Vol. 31, No. 1-3, 35-41, doi: [10.5004/dwt.2011.2389](https://doi.org/10.5004/dwt.2011.2389).
- [12] Al Nasser, W.N., Pitt, K., Hounslow, M.J., Salman, A.D. (2013). Monitoring of aggregation and scaling of calcium carbonate in the presence of ultrasound irradiation using focused beam reflectance measurement, *Powder Technology*, Vol. 238, 151-160, doi: [10.1016/j.powtec.2012.03.021](https://doi.org/10.1016/j.powtec.2012.03.021).
- [13] Baker, J.S., Judd, S.J. (1996). Magnetic amelioration of scale formation, *Water Research*, Vol. 30, No. 2, 247-260, doi: [10.1016/0043-1354\(95\)00184-0](https://doi.org/10.1016/0043-1354(95)00184-0).
- [14] Tai, C.Y., Chang, M.C., Liu, C.C., Wang, S.S.S. (2014). Growth of calcite seeds in a magnetized environment, *Journal of Crystal Growth*, Vol. 389, 5-11, doi: [10.1016/0043-1354\(95\)00184-0](https://doi.org/10.1016/0043-1354(95)00184-0).
- [15] Ravnik, J., Hribersek, M., Vogel, F., Steinmann, P. (2014). Numerical simulation of particle movement in cellular flows under the influence of magnetic forces, *International Journal of Simulation Modelling*, Vol. 13, No. 3, 300-311, doi: [10.2507/IJSIMM13\(3\)4.268](https://doi.org/10.2507/IJSIMM13(3)4.268).
- [16] Oshitani, J., Yamada, D., Miyahara, M., Higashitani, K (1999). Magnetic effect on ion-exchange kinetics, *Journal of Colloid and Interface Science*, Vol. 210, No. 1, 1-7, doi: [10.1006/jcis.1998.5952](https://doi.org/10.1006/jcis.1998.5952).
- [17] Madsen, H.E.L. (2007). Theory of electrolyte crystallization in magnetic field, *Journal of Crystal Growth*, Vol. 305, No. 1, 271-277, doi: [10.1016/j.jcrysgro.2007.04.023](https://doi.org/10.1016/j.jcrysgro.2007.04.023).
- [18] Lipus, L.C., Krope, J., Crepinsek, L. (2001). Dispersion destabilization in magnetic water treatment, *Journal of Colloid and Interface Science*, Vol. 236, No. 1, 60-66, doi: [10.1006/jcis.2000.7392](https://doi.org/10.1006/jcis.2000.7392).
- [19] Gabrielli, C., Jaouhari, R., Maurin, G., Keddam, M. (2001). Magnetic water treatment for scale prevention, *Water Research*, Vol. 35, No. 13, 3249-3259, doi: [10.1016/S0043-1354\(01\)00010-0](https://doi.org/10.1016/S0043-1354(01)00010-0).
- [20] Coey, J.M.D., Cass, S. (2000). Magnetic water treatment, *Journal of Magnetism and Magnetic Materials*, Vol. 209, No. 1-3, 71-74, doi: [10.1016/S0304-8853\(99\)00648-4](https://doi.org/10.1016/S0304-8853(99)00648-4).
- [21] Tebenihin, E.F., Gusev, B.T. (1970). Obrabotka vody magnitnym polem v teploenergetike, Energija, Moscow.
- [22] Klassen, V.I. (1982). *Omagnicivanie vodnyh sistem [Magnetization of Water Systems]*, Moscow: Khimiya, Himija, Moskva.
- [23] Szkatula, A., Balanda, M., Kopeć, M. (2002). Magnetic treatment of industrial water. Silica activation, *European Physical Journal – Applied Physics*, Vol. 18, No. 1, 41-49, doi: [10.1051/epjap:2002025](https://doi.org/10.1051/epjap:2002025).
- [24] Grutch, J.E., McClintock, J.W. (1984) Corrosion and deposit control in alkaline cooling water using magnetic water treatment at AMOCO's largest refinery, *Corrosion*, Vol. 84, No. 330, 1-26.
- [25] Grimes, S.M. (1988). Magnetic field effect on crystals, *Tube International*, Vol. (March).
- [26] Darvill, M. (1993). Magnetic water treatment, *Water and Waste Treatment*, Vol. 40 (July).
- [27] Tye, A. (1993). The magnetic treatment of water to prevent scaling, *Resource*, Vol. 1, 25-26.

- [28] Higashitani, K., Oshitani, J. (1998). Magnetic effects on thickness of adsorbed layer in aqueous solutions evaluated directly by Atomic Force Microscope, *Journal of Colloid and Interface Science*, Vol. 204, No. 2, 363-368, [doi: 10.1006/jcis.1998.5590](https://doi.org/10.1006/jcis.1998.5590).
- [29] Ohata, R., Tomita, N., Ikada, Y. (2004). Effect of a static magnetic field on ion transport in a cellulose membrane, *Journal of Colloid and Interface Science*, Vol. 270, No. 2, 413-416, [doi: 10.1016/j.jcis.2003.09.035](https://doi.org/10.1016/j.jcis.2003.09.035).
- [30] Zakharov, A.G., Maximov, A.I., Koksharov, S.A. (1996). The properties of physical effect applications under textile material treatment, In: *Proceedings of the 17th IFVTCC Congress*, Vienna, Austria, 173-176.
- [31] Lipus, L.C., Acko, B., Neral, B. (2013). Influence of magnetic water treatment on fabrics' characteristics, *Journal of Cleaner Production*, Vol. 52, 374-379, [doi: 10.1016/j.jclepro.2013.03.014](https://doi.org/10.1016/j.jclepro.2013.03.014).
- [32] Bozic, M., Lipus, L.C., Kokol, V. (2008). Magnetic field effects on redox potential of reduction and oxidation agents, *Croatica Chemica Acta*, Vol. 81, No. 3, 413-421.
- [33] Liu, Y., Jia, S., Ran, J., Wu, S. (2010). Effects of static magnetic field on activity and stability of immobilized α -amylase in chitosan bead, *Catalysis Communications*, Vol. 11, No. 5, 364-367, [doi: 10.1016/j.catcom.2009.11.002](https://doi.org/10.1016/j.catcom.2009.11.002).
- [34] Govindasamy, P., Dhandapani, S. (2007). Experimental investigation on the effect of magnetic flux to reduce emissions and improve combustion performance in a two-stroke, catalytic-coated, spark-ignition engine, *International Journal of Automotive Technology*, Vol. 8, No. 5, 533-542.
- [35] Kozic, V., Hamler, A., Ban, I., Lipus, L.C. (2010). Magnetic water treatment for scale control in heating and alkaline conditions, *Desalination and Water Treatment*, Vol. 22, No. 1-3, 65-71, [doi: 10.5004/dwt.2010.1549](https://doi.org/10.5004/dwt.2010.1549).
- [36] Edwin Raja Dhas, J., Somasundaram, K. (2013). Modeling and prediction of HAZ using finite element and neural network modeling, *Advances in Production Engineering & Management*, Vol. 8, No. 1, 13-24, [doi: 10.14743/apem2013.1.149](https://doi.org/10.14743/apem2013.1.149).
- [37] Lipus, L.C., Acko, B., Hamler, A. (2012). Magnetic device simulation modelling and optimisation for scale control, *International Journal of Simulation Modelling*, Vol. 11, No. 3, 141-149, [doi: 10.2507/IJSIMM11\(3\)3.205](https://doi.org/10.2507/IJSIMM11(3)3.205).